Available online at www.sciencedirect.com
ScienceDirect
Polymer 49 (2008) 1926–1933
polymer
www.elsevier.com/locate/polymer

Perturbing effects of bulky comonomers on the chain conformation of poly(vinylidene fluoride)

Yuning Yang [a], Suriyakala Ramalingam [a], Guolin Wu [a], Shaw Ling Hsu [a,*], Lothar W. Kleiner [b], Fuh-Wei Tang [b], Nadine Ding [b], Syed Hossainy [b]

[a] *Polymer Science and Engineering Department, University of Massachusetts, Amherst, MA 01003, United States*
[b] *Abbott Vascular Systems, Santa Clara, CA 95054, United States*

Received 3 January 2008; received in revised form 6 February 2008; accepted 8 February 2008
Available online 14 February 2008

Abstract

The comonomer effect on the structures of poly(vinylidene fluoride–hexafluoropropylene) P(VDF–HFP) copolymers was analyzed by Raman spectroscopy. The HFP content of these copolymers varies from 5% to 15%. Because of steric interactions involving the bulky HFP comonomers, the predominant chain conformation has extensively more *gauche* conformers in comparison to the neat PVDF. Based on both experimental and simulation studies, specific spectroscopic features in the 400–900 cm^{-1} region have been identified that are characteristic of irregular chain conformations elucidating the perturbing effect of HFP on the equilibrium chain statistics of PVDF in the amorphous phase. In addition, these spectroscopic features were revealed to be extremely sensitive to the relative placements of the CF_3 units with respect to other fluorine atoms along the chain.

Keywords: Amorphous; Conformation; Fluorinated

1. Introduction

Fluorinated polymers have a broad spectrum of applications. A well known polymer in this family is poly(vinylidene fluoride) (PVDF). This polymer, known for its high piezoelectric constant, is used in numerous commercial electromechanical devices such as speakers and microphones [1]. When mechanical performance is valued, this polymer also possesses toughness. Although fluorine–fluorine interactions are significant, the PVDF chain has the usual rotational isomeric states designated as *trans* or *gauche*. The relative distribution of these states associated with the multitude of crystalline forms can differ substantially depending on the processing conditions and application of an electric field [2].

PVDF homopolymer can crystallize in at least three distinct crystalline phases consisting of different chain conformations. For the α phase, the chain possesses the regular sequence of $tgtg'$ conformation. The all-*trans* (*ttt*) conformation is generally referred to as the β phase, and t_3gt_3g' is known as the γ phase [3–5]. These polymorphic structures have clearly been described in previous studies [2]. Due to its specific chain conformation in the crystalline unit cell, the polar β phase has the highest remnant polarization, thus attracting considerable attention in the polymer community [6,7]. The polar β phase can be produced by uniaxial mechanical deformation with the simultaneous application of a strong electric field [8–10]. The structural rearrangement accomplished under different processing conditions has been discussed extensively. Effects of an electric field [11–14], thermal annealing [15,16] and ultra-quenching of molten PVDF [17] have been discussed previously.

It is also known that the copolymers of PVDF with a number of other monomers can alter morphological features and create interesting structures and associated physical properties [3,4,18–20]. The focus of the present study is to elucidate the effects of hexafluoropropylene (HFP). The usual commoners used previously are generally smaller than the CF_2 units thus

* Corresponding author. Tel.: +1 413 577 1125.
E-mail address: slhsu@polysci.umass.edu (S.L. Hsu).

0032-3861/$ - see front matter © 2008 Elsevier Ltd. All rights reserved.
doi:10.1016/j.polymer.2008.02.015

reducing F–F steric interactions along the chain and enhancing formation of the truly planar zigzag structure [3,4,18–20]. Steric interference of this bulky HFP comonomer is a parameter requiring additional consideration.

This HFP comonomer is bulky, possessing a very strong dipole moment, and may significantly influence chain conformation. Although most previous studies deal with the crystalline phase, we have an interest in both the amorphous phase and the crystalline portion. P(VDF–HFP) copolymers have a broad spectrum of applications ranging from biomedical devices to lithium ion batteries [21–25]. These copolymers have received attention from the industrial and scientific communities by virtue of their appealing properties such as high solubility, low degree of crystallinity, and low T_g which improve processing. P(VDF–HFP) copolymer can expediently serve in drug release applications. The HFP content has a strong effect on the release behavior of small molecular additives as shown in Fig. 1. The drugs employed have limited miscibility in the P(VDF–HFP) copolymer and are excluded from the crystalline regions. Diffusion of the drugs depends on the dynamics of the amorphous phase and the degree of crystallinity of the samples. Therefore, characterization of the amorphous phase is crucial in controlled release analysis.

Characterization of crystalline structure in the condensed state is a well-established discipline. For polymers in solution or melt, there is a total absence of long-range order. Only a few techniques are capable of elucidating the conformational distribution of these disordered polymers [26,27]. Although the chains lack long-range order, the occupations of rotational isomeric states along the backbone can be quite different. Polarized Raman scattering, however, can be used to characterize differences in conformational distribution [28–31]. Our first study concentrated on differences in chain statistics and the resultant conformation distribution of poly(ethylene oxide) in solution or melt. In the aqueous solution, *tgt* is the dominant rotational isomeric state (~50% in the conformational distribution). In contrast, *tgg* is the dominant state (~45% in the conformational distribution) in PEO melt [28]. Simulation studies support experimental data. Without any adjustable parameters, the generated simulated spectra were in excellent agreement with experimental data [28]. We subsequently employed this technique to characterize disordered polymer chains in a variety of situations, including amorphous regions in the condensed state [28,30,32–34].

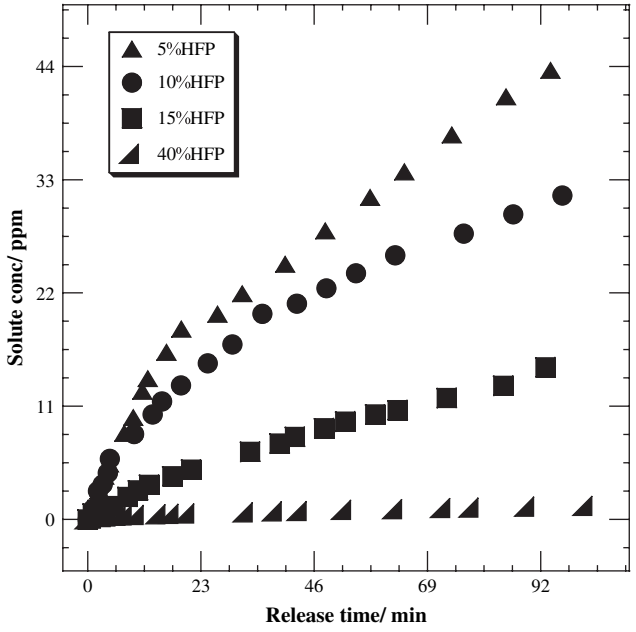

Fig. 1. Drug release from fluorinated polymeric matrix.

In this study, we employed a similar Raman technique to analyze chain conformation of PVDF incorporating different HFP contents. Based on well-established structural parameters and force constants, we have been able to establish the most probable chain conformation distributions. With polarizability parameters transferred from other molecules, it has been possible to simulate the Raman data. We found specific spectroscopic features characteristic of the perturbing effects of HFP unit to the chain conformation. Our analyses are reported here.

2. Experimental

PVDF homopolymer and P(VDF–HFP) copolymer samples of different HFP contents were obtained from Solvay (SOLEF) and 3M (Dyneon). Relative mass concentrations of HFP units in copolymers are calculated from ^{19}F NMR in DMF-d_7 and their relative reversed unit percentage also estimated from NMR spectrum. Molecular weights and their distributions are determined by GPC, utilizing DMF as solvent and polystyrene as standard. Melting temperature, heats of fusion and degree of crystallinity are estimated from differential scanning calorimetric measurements. In this study, a value of 98.0 J/g was used for the heat of fusion of the perfectly crystalline PVDF [35]. The physical properties of these samples are given in Table 1.

Raman spectra were obtained with the use of a laser confocal Raman spectrometer (Jobin Yvon HORIBA LabRam HR800 Raman microscope) in the 200–1400 cm^{-1} frequency range. Spectral resolution was maintained at 4 cm^{-1}. Laser power was ~5 mW from a He–Ne laser (632.8 nm). The incident laser was highly polarized. Polarized and depolarized spectra were obtained using a polarizer supplied by the manufacturer. As before isotropic spectra associated with the completely symmetric modes can be obtained using a linear combination of the polarized and depolarized data [31]. Using

Table 1
Physical properties of the samples studied

Sample	$M_w \times 10^3$ (g/mol)	M_w/M_n	T_m (°C)	T_g (°C)	X_c (%)
PVDF	194	1.91	174.2	−51	59
P(VDF–5%HFP)	281	1.81	161.9	−43	38
P(VDF–10%HFP)	207	1.76	160.4	−40	33
P(VDF–15%HFP)	237	1.51	135.4	−29	29

the heating cell, the Raman spectra of these samples in the molten state were obtained at temperatures just above their melting points.

Liquid-state NMR spectra were obtained using a Bruker 300 MHz spectrometer operating at 282.3 MHz at ^{19}F at room temperature. Deuterated acetone and DMF were used as solvents. $CFCl_3$ was used as the standard and given in parts per million (ppm). Solution concentration is ~1% by weight. ^{19}F NMR spectra were recorded with flip angle 30°; acquisition time 0.09 s; pulse delay 1.5 s.

Differential scanning calorimetric (DSC) measurements were conducted with a DSC 2910 differential scanning calorimeter (TA instrument Inc.). All experiments were conducted at a constant heating rate of 10 °C/min to 220 °C under nitrogen atmosphere. The temperature calibration used indium as standard.

3. Simulation of Raman spectra

Conformational analysis of amorphous chains has been challenging due to the fact that these chains do not possess periodicity. In this study, we used the program "Disordered Chain Normal Coordinate Analysis" (DCNCA) to simulate the Raman spectrum, originally developed by Snyder et al. [36,37] and modified in our laboratory. Success has been obtained for polyolefin, polyether and polyester [28,30,32–34]. The amorphous chains are represented by an ensemble of relatively short chains generated by a statistical distribution of various rotational isomeric states. The spectrum of the ensemble is used to represent the amorphous structure. A Monte Carlo method was used to generate short polymer chains based on the appropriate rotational isomeric state (RIS) model. The simulated spectra are taken to be the sum of spectra of individual chains.

$$S(v) = \sum_{i=1}^{m} S_i(v) \tag{1}$$

$$S_i(v) = \sum_{j=1}^{3n-6} I(a_j, b_j, c, v) \tag{2}$$

where $S(v)$ is the isotropic Raman spectrum (see definition below), $S_i(v)$ is the spectrum of the ith chain, m is the total number of chains considered, I is the band shape function, a is the intensity, b is the frequency of a mode, c is the half-width, j is the summation variable representing each $(3n-6)$ normal mode in a molecule with n atoms. The Raman intensities were calculated using a simple bond polarizability model [30,31,34,38]. For PVDF homopolymer and P(VDF–HFP) copolymer, the bond polarizability model includes contributions from seven sets of coordinates. They are backbone bond stretching C–C, backbone bond angle bending C_H–C_F–C_H, C_F–C_H–C_F, and the stretching C–F, bending F–C–C, F–C–F, C–C–H, where the subscripts H and F indicate the type of side atoms to which the carbon atom is connected. The scattering activity of the jth mode of a chain is given by

$$a_j = \left(\sum_{\alpha=1}^{7} A_\alpha \sum_k L_{kj}^{\alpha} \right)^2 \tag{3}$$

where A_α is an intensity parameter which is proportional to the derivative of the mean polarizability of the αth coordinate, L_{kj}^{α} is the kth element in the normal coordinate associated with the αth coordinate. The values of A_α used in the present study are 1.0, 0.8, 0.1, 0.2, 0.4, 0.5, and 0.1 for C–C, C–F, F–C–C, F–C–F, C_H–C_F–C_H, C_F–C_H–C_F and C–C–H, respectively. The force field shown in Table 2 has been transferred from previous PVDF studies and has been shown to be successful for all three PVDF crystalline forms [39].

In this experiment, a highly polarized laser is used as an excitation source. The depolarization ratio, ρ, is defined as the ratio of scattered intensity with polarization perpendicular to the scattering plane defined by the incident and scattered radiations, $I_\perp$, to the scattered intensity with polarization parallel to the polarization of the incident laser beam, $I_\parallel$. The polarizability change tensor responsible for the Raman scattering, α, can be decomposed into the isotropic part α_i and an anisotropic part α_a

Table 2
Intramolecular valence force constants of poly(vinylidene fluoride)

No.	Force constants	Coordinates involved	Common atoms	Values[a]
1	K_d	CH		4.902
2	K_R	CC		4.413
3	F_{R1}	CC, CF	C	0.403
4	F_R	CC, CC	C	0.148
5	$F_{R\gamma}$	CC, CCH	CC	0.206
6	$F_{R\omega}$	CC, CCC	CC	0.273
7	$F_{R\phi}$	CC, CCF	CC	0.567
8	F_d	CH, CH	C	0.058
9	K_1	CF		5.96
10	F_{11}	CF, CF	C	0.621
11	$F_{1\xi}$	CF, CFF	CF	0.674
12	H_γ	CCH		0.615
13	F_γ	CCH, CCH	CC	0.105
14	F_γ'	CCH, CCH	CH	0.074
15	H_δ	CHH		0.441
16	H_ω	CCC		1.248
17	f_ω^t	CCC, CCC (t)	CC	−0.036
18	H_ϕ	CCF		1.262
19	H_ξ	CFF		1.50
20	T	CCCC		0.05
21	$F_{1\phi}$	CF, CCF	CF	0.62
22	F_ϕ	CCF, CCF	CC	0.178
23	F_ϕ'	CCF, CCF	CF	0.143
24	$f_{\omega\gamma}^g$	CCC, CCH (g)	CC	0.138
25	$f_{\omega\phi}^g$	CCC, CCF (g)	CC	−0.085
26	$f_{\gamma\phi}^t$	CCH, CCF (t)	CC	0.063
27	$f_{\gamma\phi}^g$	CCH, CCF (g)	CC	0.055

[a] The stretch constants have units of mdyn/angstrom; the stretch–bend interactions have units of mdyn/rad; and the bending constants have units of (mdyn angstrom)/rad^2.

$$\alpha_{\mathrm{i}} = \frac{1}{3}(\alpha_{xx} + \alpha_{yy} + \alpha_{zz}) \tag{4}$$

$$\alpha_{\mathrm{a}} = \frac{1}{2}\Big[(\alpha_{xx} - \alpha_{yy})^2 + (\alpha_{zz} - \alpha_{yy})^2 + (\alpha_{xx} - \alpha_{zz})^2 + 6(\alpha_{xy}^2 + \alpha_{yz}^2 + \alpha_{zx}^2)\Big] \tag{5}$$

where α_{ij}s are the tensor elements. The depolarization ratio ρ is then expressed as [40]

$$\rho = \frac{I_{\perp}}{I_{\parallel}} = \frac{3(\alpha_{\mathrm{a}})^2}{45(\alpha_{\mathrm{i}})^2 + 4(\alpha_{\mathrm{a}})^2} \tag{6}$$

For an isotropic vibrational mode, α_{a} is zero, thus ρ is zero. In contrast, for an anisotropic vibration, the isotropic polarizability $\alpha_{\mathrm{i}} = 0$. In that case ρ value is 3/4. Therefore an isotropic Raman spectrum can be defined as

$$I_{\mathrm{iso}} = I_{\parallel} - \frac{4}{3} I_{\perp} \tag{7}$$

The isotropic spectrum typically is composed of conformationally sensitive skeletal modes. These modes are easy to measure and can be simulated using bond polarizability model [34,38,41].

The molecular structural parameters used in this study are shown below: the C–H, C–F and C–C bonds used were 1.096 Å, 1.34 Å and 1.54 Å, respectively. The F–C–F and H–C–H valence angles were taken as 109.5°. The C_H–C_F–C_H was taken as 118.5° and C_F–C_H–C_F as 116.5°. Torsional angles were assumed to be either *trans* ($t = 180°$), *gauche* ($g = 60°$) or *gauche′* ($g' = -60°$). The simulation methodology, structure and force field were validated by investigating experimental and simulated Raman spectra of α and β crystalline forms of PVDF homopolymer. A sample of the β form was prepared by casting films from *N*,*N*-dimethylacetamide (DMA) solution and a sample of α form was prepared by casting films from acetone solution [39]. The experimental Raman spectra of α and β forms are shown in Fig. 2. Raman simulations were then carried out for α and β forms. For β forms, all torsional angles along the backbone were set to be 180°. For the α form, torsional angles were set to be repeating sequences of *tgtg′*, where $t = 180°$, $g = 60°$ and $g' = -60°$. The simulated spectra are shown in Fig. 3. Although there is a consistent shift of 25 cm^{-1} in frequency, the experimental and simulated spectra agree quite well. A dominant band in the 800 cm^{-1} region is observed in the experimental spectra obtained for both the α and the β chains. The position of the dominant band in α form is lower than that in β form, which is also reproduced in the simulated Raman spectra. In the α form, three bands within 450–670 cm^{-1} are observed. They are reproduced in the simulated spectra. In the β form, there is only one strong band in the same region, and this feature is also reproduced in the simulation. The relative ratio of these simulated bands also agrees with the experimental results. The band at 875 cm^{-1} is absent in the simulated spectra because it is anisotropic in nature as shown in our previous study [42]. The agreement between experimental data and simulated spectra provides considerable confidence in the structure and force field employed.

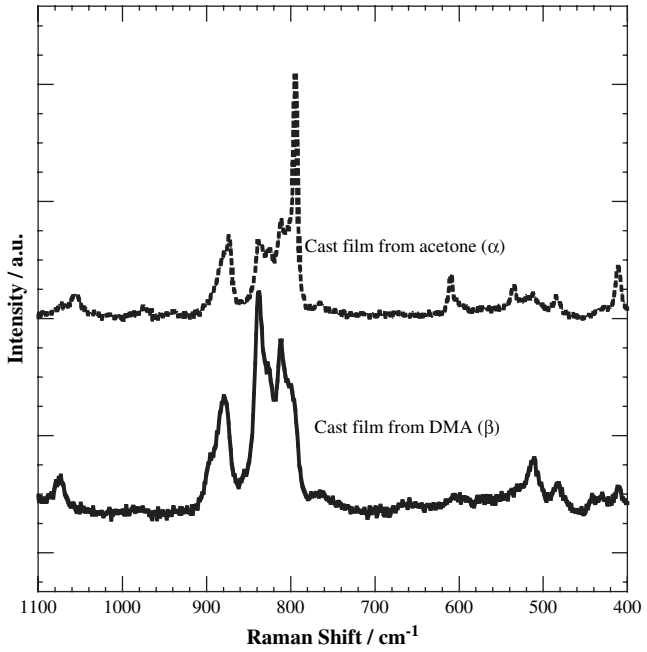

Fig. 2. Experimental Raman spectra of PVDF in α and β crystalline forms.

After investigating the PVDF homopolymer and validating the simulation methodology, Raman spectra were generated for the P(VDF–HFP) copolymer. The chain used for analysis is composed of 1 HFP unit and 13 PVDF units, corresponding to a 15 wt% of HFP content. The existence of HFP units on a PVDF chain introduces the bulky CF_3 group. Due to the steric effect of the CF_3 group, the distance L between fluorine

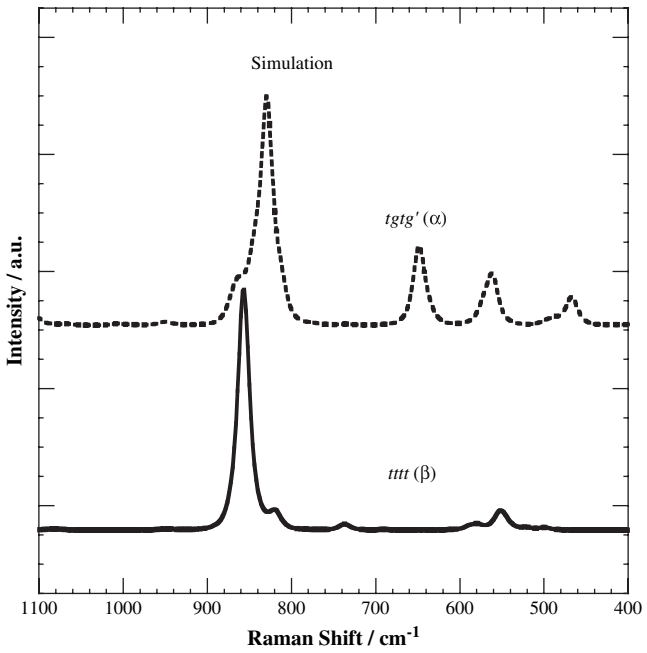

Fig. 3. Simulated Raman spectra of α and β crystalline forms of PVDF.

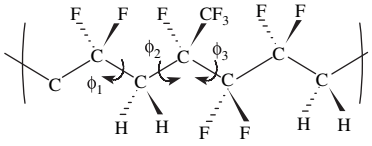

Fig. 4. Conformational structure of HFP unit.

atoms of the CF_3 group and CF_2 group in the nearest neighbor should be as large as possible. The distance L is mostly determined by the three torsional angles of the HFP unit as shown in Fig. 4. The distance L is the summation of the distance between the fluorine atoms in CF_3 groups and CF_2 groups in the HFP unit and two neighboring VDF units.

$$L = \sum_{i=1}^{3} \sum_{j=1}^{6} F_i F_j \tag{8}$$

where F_i is the three fluorine atoms in the CF_3 group and F_j is the six fluorine atoms in the three CF_2 groups. We assume that each torsional angle can take three different conformational values: t, g and g'. This distance L is calculated under all possible 27 conformational configurations. The shortest distance is 62.96 Å for the *tgt* conformation. The top three largest distances are 78.89 Å, 78.85 Å, and 77.61 Å for $gg'g$, $g'g'g$, and $tg'g$, respectively. Therefore, the most probable conformations for the HFP unit are taken to be $gg'g$, $g'g'g$, $tg'g$ in the simulation of the amorphous phase for P(VDF–HFP) copolymer.

4. Results and discussion

Determination of the copolymer configuration is an important consideration in our analysis. ^{19}F NMR spectra of one of the P(VDF–HFP) copolymers (15% HFP) in DMF-d_7 are shown in Fig. 5 and the corresponding peak assignments of the various ^{19}F NMR chemical shifts are tabulated in Table 3. Based on these observations, copolymer composition can be determined in terms of HFP content as shown below.

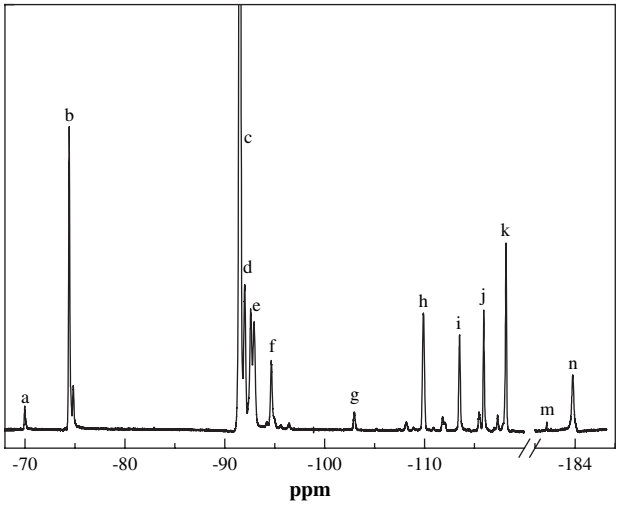

Fig. 5. ^{19}F NMR spectrum of P(VDF–HFP) copolymer with 15 wt% of HFP.

Table 3
Designations of the ^{19}F NMR chemical shifts observed for P(VDF–HFP) copolymers

No.	Assignment
a	$-CH_2-CF_2-CF(CF_3)-CF_2-$VDF
b	$-CH_2-CF_2-CF_2-CF(CF_3)-CH_2-CF_2-$
c	$-CF_2-CH_2-CF_2-CH_2-CF_2-$
d	$-CF_2-CH_2-CF_2-CF_2-CH_2-CH_2-$
e	$-CH_2-CF_2-CF_2-CF(CF_3)-CH_2-CF_2-$
f	$-CF_2-CH_2-CF_2-CH_2-CH_2-CF_2-CF_2-$
g	$-CH_2-CF_2-CF(CF_3)-CF_2-$
h	$CH_2-CF_2-CF_2-CF(CF_3)-$
i	$-CH_2-CF_2-CF_2-CH_2-CH_2-$
j	$-CH_2-CF_2-CF_2-CH_2-CH_2-$
k	$-CH_2-CF_2-CF_2-$CF(CF3)$-$
m	$-CH_2-CF_2-CF(CF_3)-CF_2-$VDF
n	$-CH_2-CF_2-CF_2-CF(CF_3)-CH_2-CF_2$

$$\text{mol ratio for } a = \text{VDF} : \text{HFP} = \frac{\frac{1}{2} I_{90-120} - \frac{1}{3}(I_a + I_b)}{\frac{1}{3}(I_a + I_b)} \tag{9}$$

$$\frac{1 \times 150}{a \times 64 + 1 \times 150} \times 100\% = \text{HFP wt\%} \tag{10}$$

where I_{90-120} is the intensity of peaks corresponding to CF_2 of VDF and HFP units and I_a and I_b are the intensities of CF_3 of HFP units. From the NMR spectra it is also possible to determine randomness of the HFP units. Based on NMR relative intensities, it is determined that most of the HFP units along the polymer chain are connected with VDF units such as $CH_2-CF_2-CF_2-CF(CF_3)-CH_2-CF_2$. Because of the steric hindrance of the bulky group CF_3, the $CF(CF_3)$ side of the HFP monomer is always connected to relatively smaller units such as CH_2. All spectroscopic evidence obtained suggests a chain configuration of random copolymers. It is reported that PVDF prepared by radical polymerization comprises 3–6% of HH or TT structures and we termed it as regio-irregular structure or reversed unit.

$$\begin{array}{c} CH_2CF_2CH_2CF_2CF_2CH_2CH_2CF_2CH_2CF_2 \\ H\ \ T\ \ H\ \ \underline{T\ T}\ \ \underline{H\ H}\ \ T\ \ H\ \ T \end{array}$$

From ^{19}F NMR spectroscopy, we calculated the reversed VDF units as around 4%. Copolymerization of HFP with VDF chains can induce various connecting patterns. For example, if we consider only three repeat units, the four probable connecting patterns in the copolymer chains are as shown below:

$CH_2CF_2CH_2CF_2CH_2CF_2$
$CH_2CF_2CF_2CH_2CH_2CF_2$
$CH_2CF_2CF_2CF(CF_3)CH_2CF_2$
$CH_2CF_2CF(CF_3)CF_2CH_2CF_2$

We can also detect the reversed HFP units in the copolymer chains by assuming $CH_2CF_2CF_2CF(CF_3)$ is the normal connecting pattern (~5% to 6%). In all spectra, the integrals of the multiplets corresponding to normal head-to-tail additions are favored (96%) over the reversed additions (head-to-head

Table 4
Calculated HFP content and regioregularity from ^{19}F NMR spectrum

Sample	Relative mol conc. of reversed VDF unit (%)	Relative mol conc. of reversed HFP unit (%)	Relative mass conc. of HFP unit
PVDF	4.1	0	0
P(VDF–5%HFP)	4.3	5.57	5.4
P(VDF–10%HFP)	4.0	5.91	10.9
P(VDF–15%HFP)	4.0	6.05	15.8

and tail-to-tail: 4%). In all spectra, most of the HFP units connected with the VDF units favor the structure: $-CH_2-CF_2-CF_2-CF(CF_3)-CH_2-CF_2-$. The calculated HFP and randomness of VDF and HFP units by ^{19}F NMR in each copolymer are shown in Table 4.

The degree of crystallinity of these samples was calculated from the heat of fusion (ΔH) obtained from DSC using the formula,

$$\%\,\chi \text{ of VDF fraction in P(VDF–HFP) copolymer} = 100 \times (X/Z) \quad (11)$$

where $X =$ experimental ΔH_{fusion} from DSC and $Z =$ average value of ΔH_{fusion} from three literature sources for PVDF, i.e. $Z \sim 98.0$ J/g [35]. In order to correct the HFP fraction in P(VDF–HFP) copolymer, the above value (Z) has been normalized to the percentage of the VDF fraction. It was observed that the addition of comonomer HFP decreased the degree of crystallinity of PVDF significantly. The degree of crystallinity was decreased as the function of HFP content while PVDF copolymerized with 40% HFP is completely amorphous. As expected, incorporation of the HFP units into PVDF chains increases the amorphous fraction.

Previous studies on poly[VDF/trifluoroethylene (TrFE)] [18–20] and poly[VDF/tetrafluoroethylene (TeFE)] [3,4] copolymers demonstrated that with increasing comonomer content, the β phase is favored. In those two copolymers, TrFE and TeFE are very minor components in the overall polymer composition. They have also been incorporated into the crystalline molecular stems [43]. The comonomers are sufficiently smaller reducing the steric interactions in the β conformation. In fact those replacements offer some relief to the CF_2-CF_2 steric hindrance in the planar zigzag chain. If the CH_2 unit is replaced by a CF_2 unit, some adjacent, non-bonded fluorine atoms would be ~0.4 Å closer than sum of their van der Waals radii (2.7 Å). Here fluorine radius was taken to be 1.35 Å and that of hydrogen to be 1.2 Å [44]. As the distance between hydrogen and fluorine is 2.3 Å, if the replacement is made an additional strain will be introduced to the α conformation. Therefore, the β phase is favored upon introduction of these small comonomers. This is not the case for the HFP comonomer. Unlike the smaller substituents, they cannot be accommodated in the crystalline units causing the degree of crystallinity to drop.

Normally, most of the Raman active backbone bond stretching and skeletal bending modes of polymers fall in the frequency range 400–1100 cm^{-1}. These modes are sensitive to the conformational change, as our previous studies have shown [28,30,32–34]. Therefore, in order to characterize the effect of HFP unit on the conformational behavior of a PVDF chain, we focused on this 400–1100 cm^{-1} frequency region. The simulation methodology, structure and force field have been validated by experimental and simulated Raman spectra of α and β crystalline forms of PVDF homopolymer as previously discussed. We then focus on the P(VDF–HFP) copolymer. The steric effect of the bulky CF_3 group should be dominant on the conformational behavior and drive the conformational structure of PVDF away from the $tgtg'$ conformer. In order to investigate the steric effect, the fluorine atoms' distance L is calculated as discussed above.

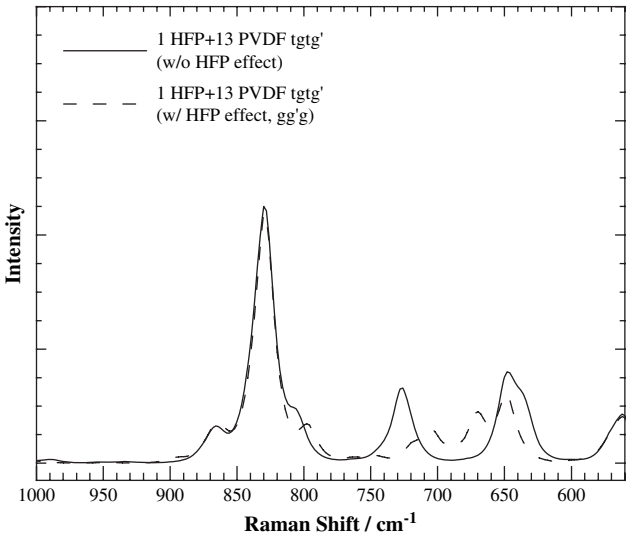

Fig. 6. Simulated Raman spectrum of P(VDF–HFP) copolymer in α conformation, with and without HFP effect.

The three most favorable states ($gg'g$, $g'g'g$, $tg'g$) found were used to analyze a copolymer with 1 HFP unit and 13 PVDF units, corresponding to 15% HFP by weight. In order to assess the HFP effect, the simulation is done for a copolymer chain with a totally α conformation sequence ($tgtg'$) and copolymer chain with α conformation for PVDF units and $gg'g$ conformation for HFP unit. The simulation results are shown in Fig. 6. It is observed that in the simulation spectrum without HFP effect, there is a band at 726 cm^{-1} which is absent in the simulation spectrum with HFP effect. For the sake of comparison, the experimental data for P(VDF–HFP) copolymer are shown in Fig. 7. It is clear that there is no band at 726 cm^{-1}. By comparing the simulation spectra with and without HFP effect to the experimental spectrum, we verify that the simulated spectrum with HFP effect more accurately describes the experimental spectrum. It is therefore concluded that due to the steric effect of the CF_3 group, the HFP unit has a strong effect on the α conformation of PVDF chain. For totally α conformation, the overall *gauche* content is 50%. When the HFP effect is considered, i.e. conformational configuration of HFP unit is taken to be $gg'g$, the *gauche* content is increased to be 57%. As we expected, the HFP unit increases the overall *gauche* population due to the steric effect of CF_3 group.

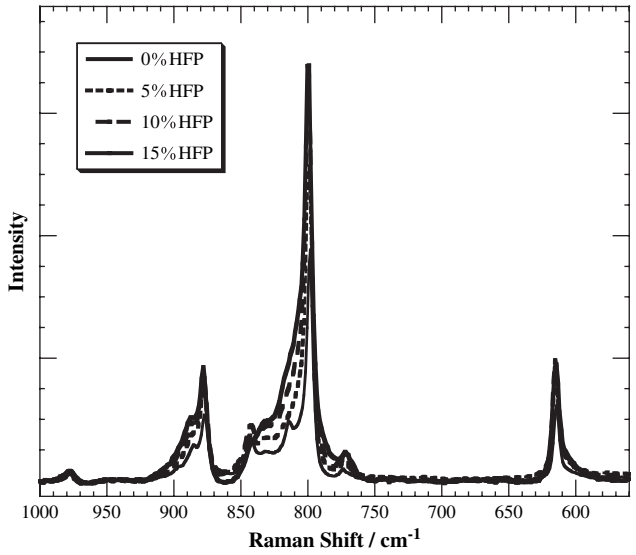

Fig. 7. Experimental Raman spectrum of P(VDF–HFP) copolymers after melt-cooled (α conformation).

After we investigate the effect of HFP on α conformation, we then focus on the amorphous phase of P(VDF–HFP) copolymer and the HFP effect on amorphous chains. In order to simulate the amorphous chains, it is necessary to know the conditional probability of conformational angle for each torsional angle along the chain. For PVDF units, we utilized the conditional probability matrices based on the model proposed by Byutner and Smith [45].

$$U_1 = \begin{pmatrix} 0.168 & 0.416 & 0.416 \\ 0.439 & 0.518 & 0.043 \\ 0.439 & 0.043 & 0.518 \end{pmatrix}$$

$$U_2 = \begin{pmatrix} 0.052 & 0.474 & 0.474 \\ 0.502 & 0.462 & 0.036 \\ 0.502 & 0.036 & 0.462 \end{pmatrix}$$

where U_1 is the matrix for torsional angle 1 and U_2 is the matrix for torsional angle 2 in PVDF unit. The $[i][j]$th element in the matrix is the statistical weight of the $[i][j]$th configuration, where i indicates the previous torsional angle and j indicates the current torsional angle. The indexes i and j range from 1 to 3 and correspond to t, g and g', respectively. In this model, the conformational energy is calculated for each configuration and the statistical weight of each configuration is derived from the energy. The overall *gauche* population in this model is ~65%. This model has been investigated and compared with other models in our previous work and supported by our spectroscopic analysis on PVDF homopolymer in the amorphous phase [42]. For the HFP unit, since the three torsional angles will arrange in a way that the distance L is as large as possible as discussed above, we take the three conformational configurations that yield the top three largest L to be the most probable. These three conformational configurations are $gg'g$, $g'g'g$, and $tg'g$ for three torsional angles ϕ_1, ϕ_2 and ϕ_3 as shown in Fig. 4. Therefore, ϕ_1 takes three values t, g and g' while ϕ_2 is always kept as g' and ϕ_3 is always kept as g. The conditional probability matrices are shown below

$$U_1 = \begin{pmatrix} 0.333 & 0.333 & 0.333 \\ 0.000 & 0.000 & 0.000 \\ 0.000 & 0.000 & 0.000 \end{pmatrix}$$

$$U_2 = \begin{pmatrix} 0.000 & 0.000 & 1.000 \\ 0.000 & 0.000 & 1.000 \\ 0.000 & 0.000 & 1.000 \end{pmatrix}$$

$$U_3 = \begin{pmatrix} 0.000 & 0.000 & 0.000 \\ 0.000 & 0.000 & 0.000 \\ 0.000 & 1.000 & 0.000 \end{pmatrix}$$

and ϕ_2, ϕ_3 are kept at fixed value. Simulation is then carried out for amorphous chains of P(VDF–HFP) copolymer. One simulation uses the assumption that all torsional angles follow the conformational probabilities of amorphous PVDF homopolymer chains including HFP unit. Another simulation considers the HFP unit so that the three torsional angles of HFP unit follow different conformational probabilities. The results are shown in Fig. 8 for comparison. Experimental Raman data for amorphous P(VDF–HFP) are shown in Fig. 9. When we compare the simulated spectra with and without the HFP effect, it is clear that a band at 710 cm^{-1} is only present when we consider the HFP effect. This 710 cm^{-1} band is also present in the experimental spectrum. Therefore, it can be concluded that consideration of the HFP effect is necessary, and the existence of the HFP unit does perturb the chain statistics of the PVDF amorphous phase. As the conformational distribution of the HFP unit is among $gg'g$, $g'g'g$, and $tg'g$, the overall *gauche* population should increase. Without the HFP effect, the *gauche* content is 65%. When the HFP effect is taken into account, the *gauche* content increases to 69%.

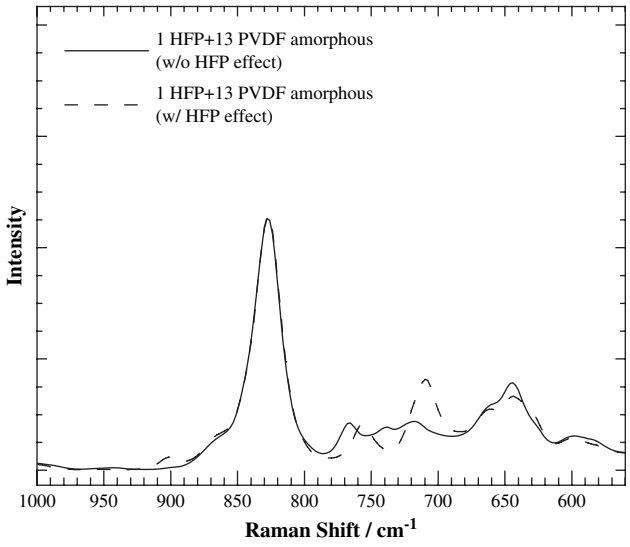

Fig. 8. Simulated Raman spectrum of P(VDF–HFP) copolymer in amorphous state, with and without HFP effect.

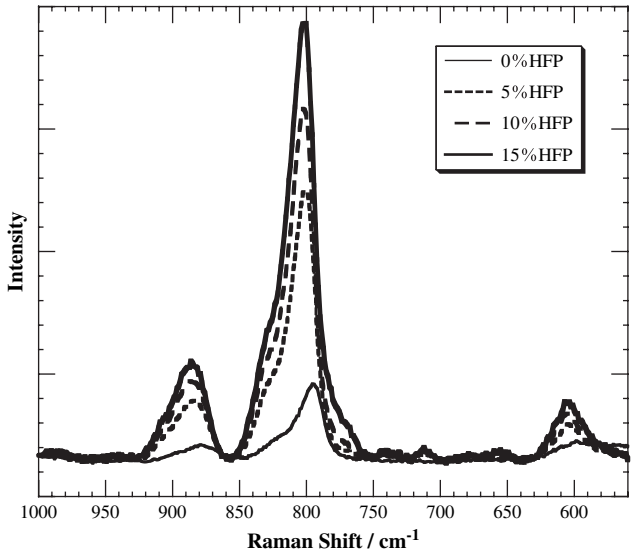

Fig. 9. Experimental Raman spectrum of P(VDF–HFP) copolymers in molten state (amorphous).

5. Conclusions

For P(VDF–HFP) copolymer, introduction of HFP comonomer affects the conformational behavior of PVDF chains. As expected, bulky CF_3 groups in HFP will significantly lower PVDF melting temperature and degree of crystallinity. Bulky HFP units cannot be accommodated in crystalline regions. Experimental Raman studies and Raman simulation have been carried out to investigate the effect of the HFP unit on α conformational sequences as well as amorphous chains of PVDF. Spectroscopic features characteristic of the perturbation on the conformational behavior of PVDF due to HFP units, which is around 700 cm^{-1} region, have been identified. In addition, it was revealed that these spectroscopic features are extremely sensitive to the relative placements of the CF_3 units with respect to other fluorine atoms along the chain. The existence of HFP units alters the conformational sequence in the α conformation, and also changes chain statistics in the amorphous phase. Due to the steric effect of the CF_3 group, the overall *gauche* population increases from 65% to 69% in the amorphous phase.

Acknowledgements

The authors gratefully acknowledge Solvay (SOLEF) and 3M (Dyneon) for providing samples for this study and also for financial support from the NSF Materials Research Science and Engineering Center at University of Massachusetts and a grant from Abbott.

References

[1] Nalwa H. Ferroelectric polymers. New York; 1995.
[2] Lovinger AJ. Developments in crystalline polymer. Springer; 1982.
[3] Lovinger AJ. Macromolecules 1983;16:1529.
[4] Broadhust MG, Davis GT, De Reggi AS, Roth SC, Collins RE. Polymer 1982;23:22.
[5] Giannetti E. Polym Int 2001;50:10.
[6] Nagai M, Nakamura K, Uehara H, Kanamoto T, Takahashi Y, Furukawa T. J Polym Sci Part B Polym Phys 1999;37:2549.
[7] Jungnickel BJ. Polymeric materials handbook. New York: CRC Press Inc.; 1996.
[8] Grecorio R, Cestari M. J Polym Sci Part B Polym Phys 1994;32:858.
[9] Hsu TC, Geil PH. J Mater Sci 1989;24(4):1219.
[10] Kaura T, Nath R, Perlman MM. J Phys D Appl Phys 1991;24:1848.
[11] Scheinbeim JI, Newman BA, Sen A. Macromolecules 1986;19:1454.
[12] Davies GR, Singh H. Polymer 1979;20:772.
[13] Sajkiewicz P. J Polym Sci Part B Polym Phys 1994;32:313.
[14] Lu FJ, Hsu SL. Macromolecules 1986;19:326.
[15] ElMohajir B-E, Heymans N. Polymer 2001;42:5661.
[16] Weinhold S, Litt MH, Lando JB. Macromolecules 1980;13:1178.
[17] Hsu CC, Geil PH. J Appl Phys 1984;56(9):2404.
[18] Oka Y, Murata Y, Koizumi N. Polym J 1986;18:417.
[19] Furukawa T, Lovinger AJ, Davis GT, Broadhust MG. Macromolecules 1983;16:1885.
[20] Kodama H, Takahashi Y, Furukawa T. Jpn J Appl Phys 1999;38:3589.
[21] Liu TY, Lin WC, Huang LY, Chen SY, Yang MC. Polym Adv Technol 2005;16(5):413.
[22] Laroche G, Marois Y, Guidoin R, King MW, Martin L, How T, et al. J Biomed Mater Res 1995;29(12):1525.
[23] Klinge U, Klosterhalfen B, Ottinger AP, Junge K, Schumpelick V. Biomaterials 2002;23(16):3487.
[24] Wu C-G, Lu M-I, Tsai C-C, Chuang H-J. J Power Sources 2006;159:295.
[25] Pu W, He X, Wang L, Jiang C, Wan C. J Membr Sci 2005;272:11.
[26] Kaji H, Schmidt-Rohr K. Macromolecules 2001;34(21):7382.
[27] Bosco M, Segre A, Miertus S, Cesaro A, Paoletti S. Carbohydr Res 2005;340(5):943.
[28] Yang X, Su Z, Wu D, Hsu SL, Stidham HD. Macromolecules 1997; 30(13):3796.
[29] Kang S, Zhang G, Aou K, Hsu SL, Stidham HD, Yang X. J Chem Phys 2003;118(7):3430.
[30] Yang X, Kang S, Hsu SL, Stidham HD, Smith PB, Leugers A. Macromolecules 2001;34(14):5037.
[31] Kang S, Hsu SL, Stidham HD, Smith PB, Leugers MA, Yang X. Macromolecules 2001;34(13):4542.
[32] Hsu SL, Hahn T, Suen W, Kang S, Stidham HD, Siedle AR. Macromolecules 2001;34(10):3376.
[33] Hahn T, Suen W, Kang S, Hsu SL, Stidham HD, Siedle AR. Polymer 2001;42(13):5813.
[34] Yang X, Kang S, Yang Y, Aou K, Hsu SL. Polymer 2004;45(12):4241.
[35] Nakagawa K, Ishida Y. J Polym Sci Part B Polym Phys 1973; 11(11):2153.
[36] Cates DA, Strauss HL, Snyder RG. J Phys Chem US 1994;98(16): 4482.
[37] Hallmark VM, Bohan SP, Strauss HL, Snyder RG. Macromolecules 1991;24(14):4025.
[38] Snyder RG, Kim Y. J Phys Chem US 1991;95(2):602.
[39] Kobayashi M, Tashiro K, Tadokoro H. Macromolecules 1975;8:158.
[40] Long DA. The Raman effect: a unified treatment of the theory of Raman scattering by molecules. New York: Wiley; 2002.
[41] Machida K, Noma H, Miwa Y. Indian J Pure Appl Phys 1988;26(2–3): 197.
[42] Yang Y, Wu G, Ramalingam S, Hsu SL. Macromolecules 2007; 40(26):9658.
[43] Lando JB. J Polym Sci Polym Lett Ed 1967;5:917.
[44] Farmer BL, Hopfinger AJ, Lando JB. J Appl Phys 1972;43:4293.
[45] Byutner OG, Smith GD. Macromolecules 1999;32(25):8376.